Applied Microbiology and Biotechnology (2024) 108:170
https://doi.org/10.1007/s00253-023-12906-5

APPLIED MICROBIAL AND CELL PHYSIOLOGY

Metabolic adaptations of *Microbacterium sediminis* YLB-01 in deep-sea high-pressure environments

Xu Qiu[1] · Xiao-Min Hu[1] · Xi-Xiang Tang[2] · Cai-Hua Huang[3] · Hua-Hua Jian[4] · Dong-Hai Lin[1]

Received: 10 July 2023 / Revised: 30 October 2023 / Accepted: 7 November 2023

Abstract

The deep-sea environment is an extremely difficult habitat for microorganisms to survive in due to its intense hydrostatic pressure. However, the mechanisms by which these organisms adapt to such extreme conditions remain poorly understood. In this study, we investigated the metabolic adaptations of *Microbacterium sediminis* YLB-01, a cold and stress-tolerant microorganism isolated from deep-sea sediments, in response to high-pressure conditions. YLB-01 cells were cultured at normal atmospheric pressure and 28 ℃ until they reached the stationary growth phase. Subsequently, the cells were exposed to either normal pressure or high pressure (30 MPa) at 4 ℃ for 7 days. Using NMR-based metabolomic and proteomic analyses of YLB-01 cells exposed to high-pressure conditions, we observed significant metabolic changes in several metabolic pathways, including amino acid, carbohydrate, and lipid metabolism. In particular, the high-pressure treatment stimulates cell division and triggers the accumulation of UDP-glucose, a critical factor in cell wall formation. This finding highlights the adaptive strategies used by YLB-01 cells to survive in the challenging high-pressure environments of the deep sea. Specifically, we discovered that YLB-01 cells regulate amino acid metabolism, promote carbohydrate metabolism, enhance cell wall synthesis, and improve cell membrane fluidity in response to high pressure. These adaptive mechanisms play essential roles in supporting the survival and growth of YLB-01 in high-pressure conditions. Our study offers valuable insights into the molecular mechanisms underlying the metabolic adaptation of deep-sea microorganisms to high-pressure environments.

Key points

- *NMR-based metabolomic and proteomic analyses were conducted on Microbacterium sediminis YLB-01 to investigate the significant alterations in several metabolic pathways in response to high-pressure treatment.*
- *YLB-01 cells used adaptive strategies (such as regulated amino acid metabolism, promoted carbohydrate metabolism, enhanced cell wall synthesis, and improved cell membrane fluidity) to survive in the challenging high-pressure environment of the deep sea.*
- *High-pressure treatment stimulated cell division and triggered the accumulation of UDP-glucose, a critical factor in cell wall formation, in Microbacterium sediminis YLB-01 cells.*

Keywords *Microbacterium sediminis* · Metabolic adaptation · High-pressure conditions · Metabolomics · Proteomics

✉ Xi-Xiang Tang
tangxixiang@tio.org.cn

✉ Dong-Hai Lin
dhlin@xmu.edu.cn

[1] Key Laboratory for Chemical Biology of Fujian Province, MOE Key Laboratory of Spectrochemical Analysis and Instrumentation, College of Chemistry and Chemical Engineering, Xiamen University, Xiamen, China

[2] State Key Laboratory Breeding Base of Marine Genetic Resources, Key Laboratory of Marine Genetic Resources, Fujian Key Laboratory of Marine Genetic Resources, Third Institute of Oceanography, Ministry of Natural Resources, Xiamen, China

[3] Research and Communication Center of Exercise and Health, Xiamen University of Technology, Xiamen, China

[4] State Key Laboratory of Microbial Metabolism, School of Life Sciences and Biotechnology, Shanghai Jiao Tong University, Shanghai, China

Published online: 24 January 2024

Introduction

The deep sea, which encompasses water depths of over 1000 m, constitutes nearly half of the Earth's surface and three-quarters of the total ocean area (Fang et al. 2010). This vast and self-contained ecosystem has a high level of biodiversity, and is crucial for the planet's productivity (Simmons et al. 2008). Microorganisms living in the deep sea have developed specialized metabolic adaptations to cope with extreme environments (Simonato et al. 2006). Compared to their terrestrial counterparts, deep-sea microorganisms face a myriad of environmental stressors (Sogin et al. 2006). In recent years, research has uncovered some of the adaptive strategies used by deep-sea microorganisms to survive extreme conditions such as low temperatures, anaerobic environments, and oligotrophic conditions (Ohmae et al. 2015; Parrilli et al. 2021; Xie et al. 2018). However, the survival strategies of these microorganisms are not yet well understood.

The deep-sea environment is characterized by the high hydrostatic pressures (up to 110 MPa, Mariana Trench), covering a significant portion of the marine ecosystem and presenting a formidable challenge (Abe and Horikoshi 2001). Research has clarified the molecular mechanisms used by microbes to withstand high-pressure conditions, including the regulation of gene and protein expression (Campanaro et al. 2005; Ishii et al. 2005), alterations in flagellar movement (Jian et al. 2016), enhancement of anaerobic respiration (Xiao et al. 2007), accumulation of trimethylamine N-oxide (TMAO) (Qin et al. 2021), reduction of antioxidant stress (Xie et al. 2018), and adjustment of unsaturated fatty acid proportions in cell membranes (Delong and Yayanos 1986; Oger and Jebbar 2010). However, a comprehensive understanding of how deep-sea microorganisms adapt to the simultaneous challenges of high pressure and low temperature necessitates a thorough investigation of their metabolic characteristics. By examining their metabolic profiles, we can gain valuable insights into their adaptive strategies and mechanisms.

Within the genus of *Microbacterium*, valuable secondary metabolites have been identified. Notably, an actinomycete strain, *Microbacterium sediminis* YLB-01 (MCCC 1A06153 = DSM 23767), was isolated from deep-sea sediments in the southwestern Indian Ocean (49.8405° E 37.8111° S) at a depth of 2327 m (Yu et al. 2013). This strain exhibited tolerance to both low temperatures (LT) and high hydrostatic pressures (HP) (Yu et al. 2013). To gain further insights into the effects of LT and HP on YLB-01 cells, we performed a comprehensive transcriptomic analysis, which revealed significant effects on key biological processes such as cell division, DNA damage repair response, energy metabolism, amino acid metabolism, fatty acid metabolism, and more (Qiu et al. 2022).

High-pressure environments in the deep sea present unique challenges, especially when combined with low temperatures. In our previous study, we conducted an NMR-based metabolomic analysis of YLB-01 cells cultivated at low temperature (LT) and normal temperature (NT) under high pressure, comparing their metabolic profiles (LTHP *vs.* NTHP). Simultaneously, the effects of high pressure (under low temperature, HPLT *vs.* NPLT) on metabolic patterns were briefly described (Xia et al. 2020). These results highlight the significant influence of temperature and growth phase on the metabolic adaptations of YLB-01 cells under high- pressure conditions. However, the specific mechanisms by which the deep-sea YLB-01 strain adapts to high-pressure conditions at low temperature remain largely unexplored. Investigating the metabolic changes exhibited by YLB-01 cells under high pressure (HP) compared to normal pressure (NP) at low temperature could significantly enhance our understanding of the adaptations of the YLB-01 strain to high-pressure conditions.

The aim of this study was to elucidate the metabolic differences in YLB-01 cells under high-pressure conditions compared to normal pressure conditions at low temperature (HPLT *vs*. NPLT), and to determine the molecular basis for the adaptation processes of the YLB-01 strain in high-pressure environments. By using NMR-based metabolomic analysis and proteomic analysis, we conducted a comprehensive investigation including changes in metabolite concentration and protein expression, regulation of metabolic profile and pathway, and other adjustments involved in the adaptation of YLB-01 cells to high-pressure conditions. Our results shed new light on the complex adaptation mechanisms used by deep-sea microorganisms to survive in the challenging high-pressure environments.

Materials and methods

Strain information and cultural conditions

A single colony of the *Microbacterium sediminis* YLB-01 (MCCC 1A06153 = DSM 23767) strain was inoculated from an agar plate into individual test tubes containing 5 mL of tryptone soy broth (TSB) medium. The test tubes were then incubated in a shaker at 28 °C for 12 h. Subsequently, the seed cultures were transferred to 150-mL Erlenmeyer flasks at a ratio of 1:20, with each flask containing 100 mL of TSB medium.

We created specific culture conditions to imitate the challenging conditions of the deep-sea high-pressure environment, such as 30 MPa at 4 °C (high pressure and low temperature, HPLT) and 0.1 MPa at 4 °C (normal pressure

and low temperature, NPLT). To ensure an adequate cell number, YLB-01 cultures were initially cultured under optimal conditions (28 °C, 0.1 MPa) for 24 h. The optical density at 600 nm ($OD_{600\ nm}$) of the cell cultures was measured using an automatic growth curve analyzer (FP-1100-C, Growth Curves Ab Ltd., Finland). Once the cultures reached the stationary growth phase, the cells were transferred into a 100-mL sterile saline bag and placed in a high-pressure culture kettle. This kettle, obtained from Nantong Feiyu Company, China, was specifically designed to simulate the high-pressure conditions of the deep sea (Zhang et al. 2015). The cells were then exposed to either 30 MPa (the HPLT group, N = 8) or 0.1 MPa (the NPLT group, N = 7) at 4 °C for 7 days. Hydrostatic pressure was created by injecting deionized water into the vessel. The pressure increased immediately within a few seconds, ensuring that the cells were alive.

Aqueous metabolite extraction

Following the culturing of the YLB-01 cells, 100 mL of the culture was placed into a 250-mL centrifuge bottle and then centrifuged at 4 °C (6000 g, 5 min). The supernatant was carefully decanted, and the cell pellets were rapidly cooled to -40 °C using 100 mL of a buffer composed of a 3:2 methanol/water mixture containing 0.85% (wt/vol) NaCl. The mixture was centrifuged again at 4 °C (6000 g, 5 min). The cell pellets were washed three times with 5 mL of cold phosphate-buffered saline (PBS) and centrifuged at 4 °C (6000 g, 5 min) after each wash. Finally, the cell pellets were stored at -80 °C until further use.

Aqueous metabolites were extracted from the frozen cell pellets according to a previously described protocol (Ye et al. 2012). Initially, 600 µL of a cold extraction buffer consisting of a 1:1 mixture of distilled water and acetonitrile was added to homogenize the samples. The mixtures were then sonicated on wet ice for 180 cycles, with each cycle consisting of 2 s of ultrasound followed by a 3-s pause, and then centrifugation at 4 °C (12,000 g, 10 min). To harvest metabolites from the residues, 600 µL of extraction solution was added and then the samples were centrifuged a second time. The supernatants were collected and lyophilized, resulting in an extract powder that was stored at -80 °C for further analysis.

Sample preparation for NMR-based metabonomics analysis

The lyophilized extract powder of YLB-01 cells was dissolved in 550 µL of phosphate buffer [50 mM K_2HPO_4/NaH_2PO_4, 10% (v/v) D_2O, 1 mM 3-(Trimethylsilyl) propionate-2,2,3,3-d4 acid sodium salt (TSP), pH 7.4] to prepare the NMR samples. After vigorous mixing, the samples were centrifuged at 4 °C (12,000 g, 15 min) to remove any insoluble components. Clear supernatant aliquots were then transferred to 5-mm NMR tubes for further analysis.

NMR experiments

All NMR experiments were performed on the samples prepared from YLB-01 cells with a Bruker Avance III 600 MHz spectrometer (Bruker BioSpin, Germany) at a temperature of 25 °C. 1D ^{1}H NOESY spectra were recorded using the pulse sequence noesygppr1d [(RD)-90°-t_1-90°-τ_m-90°-ACQ]. Water suppression was achieved by irradiating the water resonance during the recycle delay (RD) of 4.0 s. The short delay t_1 was set to 4.0 µs, and the mixing time τ_m was 100 ms. The spectral width was set to 16 ppm, the acquisition time ACQ was 2 s and 32 transients were collected into 64 K data points for each spectrum.

NMR data processing and analysis

The ^{1}H-NMR spectra were processed using the MestReNova program. The FID (Free Induction Decay) signal was subjected to window function processing with a line broadening of 0.30 Hz and Fourier transformed. Manual adjustments were made for baseline and phase corrections, and the chemical shifts were calibrated using TSP (0.00 ppm) as a reference. To minimize the impact of imperfect water suppression, water resonances between δ 4.70–5.10 ppm were excluded from further analysis. The NMR spectrum was segmented using a binning size of 0.001 ppm.

For data normalization, the NMR integrals were normalized by the sum of the integrals using the MATLAB program (version 2020a). This approach accounted for any discrepancies in cell numbers between samples.

Resonance assignments of aqueous metabolites were performed based on the ^{1}H-NMR spectra using the Chenomx NMR Suite 8.3 (Chenomx Inc, Canada), the HMDB database (https://hmdb.ca/), and relevant references. The Chenomx NMR Suite facilitated the identification of metabolites by comparing their spectral patterns with the reference spectra stored in the database. Additionally, the HMDB database served as a valuable resource for confirming the identity of metabolites based on their chemical shifts and other spectral features.

Univariate statistical analysis

Data analysis was performed using the IBM SPSS 19 software. Student's t-test was used to identify metabolites with significant concentration differences between the HPLT and NPLT groups. The results were presented as mean ± SD. Statistical significance was as follows: $p > 0.05$ (ns), $p < 0.05$ (*), $p < 0.01$ (**), $p < 0.001$ (***) and $p < 0.0001$ (****).

Metabolites with a p-value < 0.05 were considered as differential metabolites.

Multivariate statistical analysis

The normalized NMR spectral data were imported into the SIMCA software (MKS Umetrics, Sweden, version 14.0) and subjected to Pareto-scaling to balance the influence of different metabolites. To gain a comprehensive understanding of the data, various multivariate statistical analyses were performed, including principal component analysis (PCA), partial least squares discriminant analysis (PLS-DA), and orthogonal partial least squares discriminant analysis (OPLS-DA). PCA provided an overview of the inherent patterns and clustering in the data, while PLS-DA and OPLS-DA maximized the separation between the metabolic profiles of different groups.

To assess the reliability of the OPLS-DA model, a response permutation test with 200 cycles was conducted. In this test, class assignments of the samples were randomized multiple times to establish a null distribution and assess the predictive ability of the model. The resulting cross-valuation plot provided insight into the robustness of the model.

Metabolites with a Variable Importance in Projection (VIP) value > 1 were identified as significant metabolites. The combination of univariate and multivariate statistical analyses was used to identify characteristic metabolites, with p-value < 0.05 and VIP > 1. This integrated approach helped in determining the metabolites that exhibited both statistical significance and relevance to the metabolic differentiation between groups.

Metabolic pathway analysis

Metabolic pathway analysis was conducted using MetaboAnalyst, an online server (https://new.metaboanalyst.ca/MetaboAnalyst/), to screen significantly altered metabolic pathways that exhibited significant alterations under high-pressure conditions. Pathway topological analysis (PTA) was implemented to calculate the pathway impact value (PIV) for each metabolic pathway. PIV was determined by adding the importance measures of the matched metabolites and then dividing by the sum of the importance measures of all metabolites in the pathway. The PIV and PTA can depict metabolic pathways variability and complex networks. The higher the PIV, the more important the pathway is to the metabolic network. Both PIV > 0.1 and p-value < 0.05 were used as screening criteria. These thresholds helped identify significant metabolic pathways that had a substantial impact and were statistically significant in relation to the high-pressure conditions.

Sample preparation for proteomics analysis

For proteomics analysis, YLB-01 cells were harvested by centrifugation at 4 °C (6000 g, 5 min). Each of the NPLT and HPLT groups consisted of three samples to ensure statistical robustness. The harvested cell pellets were used for sample preparation for proteomics analysis.

Initially, each sample was supplemented with 400 µL of SDT lysate and subjected to treatment in a boiling water bath for 5 min. The resulting cell pellets were then shock disrupted and further treated in a boiling water bath for 15 min. Ultrasonic disruption was performed, followed by centrifugation at 12,000 g for 30 min. The resulting supernatant was collected, and protein quantification was carried out using the BCA assay.

Next, 100 µg of protein was taken and combined with DTT (dithiothreitol) to achieve a final concentration of 100 mM. The mixture was boiled in a water bath for 5 min and subsequently cooled to room temperature. Then 200 µL of UA buffer (8 M urea, 150 mM Tris–HCl, pH 8.0) was added to the sample and thoroughly mixed. The mixture was centrifuged in a 10-kDa ultrafiltration tube at 14,000 g for 30 min. This centrifugation step was repeated by adding a further 200 µL of UA buffer and discarding the filtrate. Then, 100 µL of IAA (iodoacetamide, 50 mM in UA) was added, and the mixture was vortexed at 600 rpm for 1 min. The sample was then kept at room temperature for 30 min while being protected from light. Further centrifugation was carried out at 14,000 g for 30 min, repeating this centrifugation process twice by adding 100 µL of UA buffer and centrifuging at 14,000 g for 30 min each time. Subsequently, 100 µL of NH_4HCO_3 buffer was added, and the mixture was centrifugated at 14,000 g for 30 min, repeated this step twice.

To facilitate protein digestion, 104 µL of trypsin buffer (containing 2 µg trypsin in 1040 µL of NH_4HCO_3 buffer) was added to the sample, and the mixture was vortexed at 600 rpm for 1 min. The sample was then incubated at 37 °C for 16–18 h to allow complete digestion. After the digestion period, the sample was centrifuged at 14,000 g for 30 min to collect the filtrate. The obtained filtrate was desalted using a C18-SD extraction disc cartridge, and the protein content was quantified by measuring the OD value at 280 nm.

LC–MS/MS-based proteomics analysis

LC–MS/MS experiments were performed on the samples prepared from YLB-01 cells to analyze the enzymatic hydrolysis products. The hydrolysates were separated using an EASY-nLC 1000 nL flow rate HPLC liquid phase system. The system used two liquid phases: liquid A, consisting of a 0.1% formate-acetonitrile aqueous solution (acetonitrile, 2%); liquid B consisting of a 0.1% acetonitrile aqueous solution (acetonitrile, 84%). The EASY column SC001

(150 µm × 20 mm, RP-C_{18}) was used as a trap column and the Thermo EASY column SC200 (150 µm × 100 mm, RP-C_{18}) as a separation column.

The hydrolysates were separated by capillary high-performance liquid chromatography and subjected to mass spectrometric analysis using a Q-Exactive mass spectrometer (Thermo Finnigan) operating in positive ion mode. The ion scan range was set from 300 to 1800 m/z, and MS^2 scans were performed to obtain fragmentation data for the identification and characterization of the hydrolysis products.

The mass spectrometry proteomics data have been deposited to the ProteomeXchange Consortium (http://proteomecentral.proteomexchange.org) via the iProX partner repository (Ma et al. 2019) with the dataset identifier PXD044055.

Label-free analysis

The relative abundances of the enzymatic hydrolysis products in YLB-01 cells were quantified using label-free analysis with the MaxQuant software (version 1.3.0.5) for accurate quantitative analysis. To ensure reliable results, a false discovery rate (FDR) threshold of less than 0.01 was applied during the analysis to maintain high confidence. The obtained search files underwent additional processing using the Perseus software (version 1.3.0.4) for subsequent statistical analysis, including normalization and data filtering, to enhance data quality and reduce noise. Differentially expressed proteins were identified with the criterion of p-value < 0.05.

Subcellular localization analysis

Subcellular localization analysis provided insights into the distribution of these differentially expressed proteins in YLB-01 cells. We used two online servers to predict the subcellular localization: PSORTb (version 3.0.2, available at https://www.psort.org/psortb/) and CELLO (available at http://cello.life.nctu.edu.tw/). These servers provided information about the identified proteins to help interpret their functional roles and potential cellular mechanisms. By utilizing these prediction tools, we gained a better understanding of the subcellular localization patterns of the differentially expressed proteins and their potential involvement in specific cellular processes.

Multiomics analysis

Multiomics analysis was performed to address changes in metabolite concentrations and protein expression levels in YLB-01 cells. To identify the metabolites and proteins of interest, we searched for their corresponding KO numbers on the Kyoto Encyclopedia of Genes and Genomes (KEGG) database website (https://www.kegg.jp/), a comprehensive resource for biological pathway information. The collected data were then imported into the KEGG Mapper function page (https://www.genome.jp/kegg/tool/map_pathway2.html) for pathway mapping and organization of the metabolites based on their involvement in these pathways.

Using the KEGG database and mapping tools, we were able to gain insight into the metabolic pathways underlying the observed changes in metabolite concentrations and protein expression levels. This comprehensive approach allowed for a systematic examination of these pathways, highlighting their interconnectivity and identifying key metabolites and proteins associated with the biological processes under investigation. The integration of multiomics analysis with pathway analysis provided a deeper understanding of the molecular mechanisms and regulatory networks involved, contributing to the interpretation of the observed experimental results.

Results

NMR spectra of YLB-01 cells and resonance assignments of aqueous metabolites

We recorded the 600 MHz 1D ^{1}H-NMR spectra on aqueous extracts from YLB-01 cells (Fig. 1), and then assigned resonances of 31 metabolites. These metabolites were categorized into four distinct classes: amino acid metabolism (15 metabolites), carbohydrate metabolism (10 metabolites), nucleotide metabolism (4 metabolites), and energy metabolism (2 metabolites), as outlined in Supplementary Table S1. The metabolites covered a wide range of biochemical classes, playing varying roles in the metabolic profile of YLB-01 cells exposed to high-pressure conditions, and thereby revealing potential changes and essential pathways involved in sustaining cellular equilibrium.

Comparison of metabolite concentrations between the HPLT and NPHT groups

Univariate statistical analysis was used to compare the concentrations of metabolites between the HPLT and NPHT groups of YLB-01 cells during the stationary growth phase (Table 1). A total of 21 metabolites with p-value < 0.05 were identified as differential metabolites. Most of these differential metabolites were related to amino acid metabolism, including alanine, aspartate, histidine, isoleucine, leucine, lysine, methionine, phenylalanine, proline, serine, threonine, and tyrosine. Furthermore, some of differential metabolites were associated with carbohydrate metabolism, such as acetate, formate, lactate, trehalose, UDP-glucose (UDPG), and UDP-glucuronate. In addition, three differential metabolites

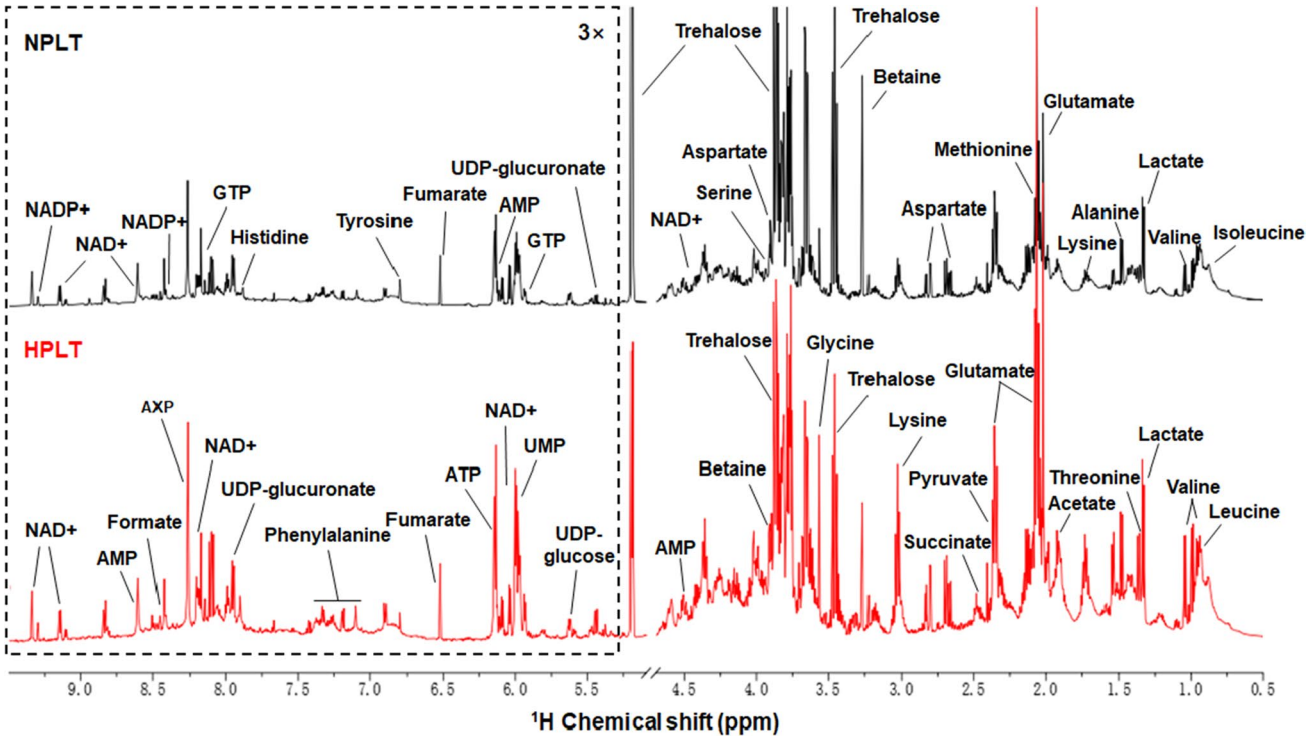

Fig. 1 Averaged 1D ^{1}H-NMR spectra recorded on aqueous extracts derived from the HPLT and NPLT groups of YLB-01 cells. The NMR spectra were recorded on a 600 MHz NMR spectrometer at 25 ℃. The vertical scales were kept constant cross the two spectra. The displayed region spans from 0.50 to 9.50 ppm, excluding the resonance region of 4.70–5.10 ppm (associated with water). To enhance clarity, the resonance region of 4.85–9.50 ppm has been magnified threefold in comparison to the region of 0.50–4.70 ppm

were linked to nucleotide metabolism, including ATP, GTP, and UMP.

These results highlight the dynamic alterations occurring in several metabolic pathways within YLB-01 cells under high-pressure conditions. The observed alterations in amino acid, carbohydrate, and nucleotide metabolisms suggest adaptive responses to maintain cellular homeostasis and energy production. The reprograming of the metabolism enables YLB-01 cells to survive in the high-pressure environments.

Metabolic changes in YLB-01 cells exposed to high-pressure conditions

Multivariate statistical analysis revealed significant metabolic changes occurring in YLB-01 cells exposed to high-pressure conditions. The PCA scores plot clearly showed distinct metabolic profiles between the HPLT and NPLT groups, with all samples falling within the 95% confidence interval (Fig. 2A). This plot highlighted the significant effect of high-pressure treatment on the metabolic profile of YLB-01 cells. In additional, the PLS-DA and OPLS-DA scores plots further reinforced the clear differentiation between the two groups, visually depicting the metabolic separation between the HPLT and NPLT groups (Fig. 2B, C).

We performed a response permutation test and obtained the following statistical parameters: R^2Y (cum) = 0.988, Q^2Y (cum) = 0.974 (Fig. 2D), indicating the high reliability of the OPLS-DA model. The response permutation plot provided further confirmed the significance of the observed metabolic differences.

Overall, the multivariate statistical analysis revealed significant changes in the metabolic profile of YLB-01 cells under high-pressure conditions. The distinct metabolic separation between the HPLT and NPLT groups highlighted the significant effect of high-pressure treatment on the metabolism of YLB-01 cells. These results highlight the adaptive responses and metabolic reprogramming that occur in YLB-01 cells exposed to high-pressure conditions.

Identification of significant metabolites and characteristic metabolites

From the OPLS-DA analysis of the HPLT *vs*. NPLT groups, we identified six significant metabolites (Table 2): lysine, serine, and threonine, which are associated with amino acid metabolism; lactate, acetate, and trehalose, which are associated to carbohydrate metabolism. Furthermore, we also identified six characteristic metabolites and ranked them according to their VIP values (Table 2,

Table 1 Quantitative comparisons of metabolite concentrations between the HPLT and NPLT groups of YLB-01 cells during the stationary growth phase

Metabolite	Mean ± SEM		Significance
	NPLT	HPLT	HPLT *vs.* NPLT
Amino acid metabolism			
alanine	0.277 ± 0.022	0.321 ± 0.011	***
betaine	0.305 ± 0.094	0.350 ± 0.135	ns
aspartate	0.198 ± 0.008	0.235 ± 0.012	****
glutamate	0.328 ± 0.062	0.319 ± 0.038	ns
glycine	0.263 ± 0.024	0.280 ± 0.006	ns
histidine	0.081 ± 0.005	0.098 ± 0.005	****
isoleucine	0.103 ± 0.007	0.121 ± 0.004	****
leucine	0.360 ± 0.024	0.427 ± 0.012	****
lysine	0.195 ± 0.012	0.349 ± 0.062	***
methionine	0.283 ± 0.014	0.334 ± 0.008	****
phenylalanine	0.024 ± 0.003	0.029 ± 0.004	**
proline	0.135 ± 0.010	0.166 ± 0.007	****
serine	0.381 ± 0.036	0.511 ± 0.025	****
threonine	0.325 ± 0.031	0.448 ± 0.015	****
tyrosine	0.082 ± 0.009	0.104 ± 0.010	***
valine	0.131 ± 0.008	0.163 ± 0.009	****
Carbohydrate metabolism			
acetate	0.237 ± 0.020	0.341 ± 0.020	****
formate	0.034 ± 0.005	0.042 ± 0.006	*
fumarate	0.058 ± 0.002	0.051 ± 0.010	ns
lactate	0.451 ± 0.010	0.552 ± 0.037	****
pyruvate	0.285 ± 0.049	0.288 ± 0.031	ns
succinate	0.125 ± 0.024	0.127 ± 0.013	ns
trehalose	1.691 ± 0.233	0.401 ± 0.048	****
UDP-glucose	0.077 ± 0.013	0.104 ± 0.019	**
UDP-glucuronate	0.023 ± 0.001	0.041 ± 0.014	**
Nucleotide metabolism			
AMP	0.132 ± 0.016	0.137 ± 0.020	ns
ATP	0.038 ± 0.006	0.050 ± 0.007	**
GTP	0.058 ± 0.004	0.072 ± 0.005	****
UMP	0.057 ± 0.006	0.069 ± 0.004	***
Energy metabolism			
NAD +	0.083 ± 0.013	0.072 ± 0.011	ns
NADP +	0.033 ± 0.002	0.034 ± 0.007	ns

Statistical significances of differences in metabolite concentration were analyzed by independent sample *t*-test: ns, $p > 0.05$; *, $p < 0.05$; **, $p < 0.01$; ***, $p < 0.001$; ****, $p < 0.0001$. Red, increase in metabolite concentration; blue, decreases in metabolite concentration

identical to the significant metabolites). These metabolites, in descending order of VIP values, were trehalose, lactate, lysine, serine, threonine, and acetate. Trehalose stood out with the highest VIP value among the metabolites, and its level was much significantly decreased in YLB-01 cells exposed to high-pressure conditions (Table 1).

These results highlight the metabolites that play a critical role in distinguishing the HPLT and NPLT groups and provide insight into the key metabolic features associated with high-pressure treatment.

Significantly altered metabolic pathway analysis

Several metabolic pathways were significantly altered in YLB-01 cells subjected to high-pressure treatment. Specifically, the carbohydrate metabolism pathways were significantly altered, including glycolysis/gluconeogenesis, pyruvate metabolism, and glyoxylate and dicarboxylate metabolism. In additional, the amino acid metabolism pathways, such as aminoacyl-tRNA biosynthesis, valine, leucine and isoleucine biosynthesis, and cysteine and methionine metabolism, also showed significant changes (Fig. 3). Aminoacyl-tRNA biosynthesis was associated with activated protein synthesis. These results highlight the effect of high-pressure conditions on key metabolic pathways and shed light on the specific biochemical processes affected by the environmental stress.

Annotation and functional analysis of peptide sequences

The label-free analysis detected and qualified 1479 peptide fragments in YLB-01 cells, with 1082 peptide fragments were annotated on the YLB-01 cell genome. We found that the expression of almost all of these annotated proteins were altered in YLB-01 cells exposed to high-pressure conditions, including 488 upregulated proteins and 594 down-regulated proteins. Notably, the high-pressure treatment altered the expression of some proteins, which were closely related to the life process of YLB-01 cells, including the proteins associated with cell division, peptidoglycan biosynthesis, amino acid metabolism, and so on (Supplementary Table S2).

Identification and functional annotation of differentially expressed proteins

A total of 379 proteins were identified as differentially expressed proteins (DEPs) based on the criterion of $p < 0.05$, including 150 upregulated proteins and 229 down-regulated proteins (Fig. 4A). The fold changes (FCs) of the DEPs were calculated, and it was found that among the upregulated DEPs, the number of DEPs with $FC > 2.00$, $1.50 < FC < 2.00$, and $1.00 < FC < 1.50$ were 19 (12.67%), 54 (36.00%), and 77 (51.33%), respectively; for down-regulated DEPs, the numbers of DEPs with $FC < 0.50$, $0.50 < FC < 0.67$, and $0.67 < FC < 1.00$ were 49 (21.40%), 85 (37.12%), and 95 (41.48%), respectively. The DEP heatmaps showed that the NPLT and HPLT samples appeared to be well clustered. The protein expression of YLB-01 cells

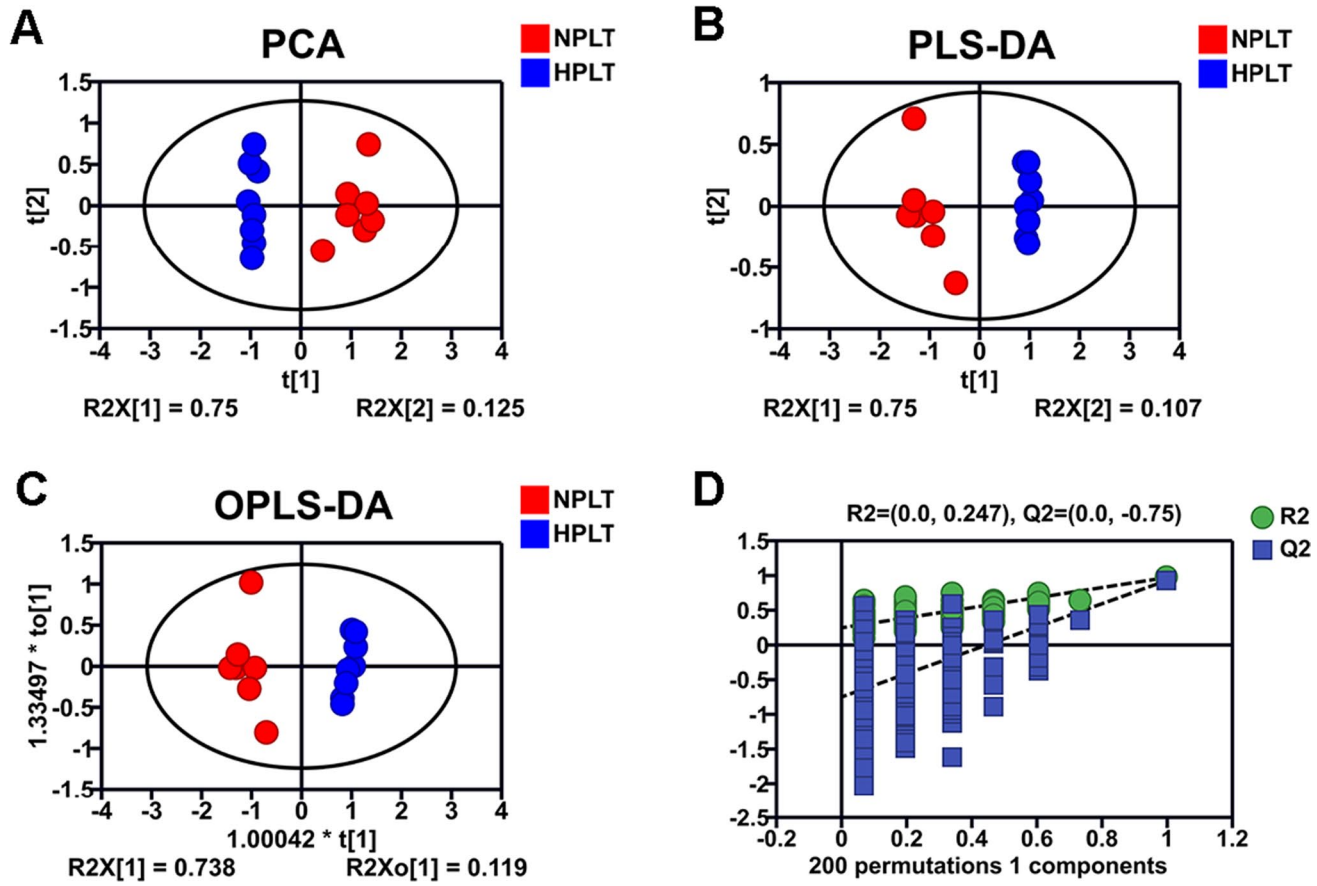

Fig. 2 Multivariate statistical analyses for NMR data from the HPLT and NPLT groups of YLB-01 cells. (**A**-**C**) Scores plots of PCA, PLS-DA and OPLS-DA models of HPLT *vs.* NPLT, (**D**) Cross-validation plot of the OPLS-DA model

Table 2 Significant metabolites and characteristic metabolites identified from the OPLS-DA analysis of the HPLT group *vs.* the NPLT group

Metabolite	VIP	HPLT *vs.* NPLT	significant metabolites	characteristic metabolites
Trehalose	4.086	↓↓↓↓	√	√
Lactate	1.409	↑↑↑↑	√	√
Lysine	1.370	↑↑↑	√	√
Serine	1.275	↑↑↑↑	√	√
Threonine	1.251	↑↑↑↑	√	√
Acetate	1.130	↑↑↑↑	√	√

Statistical significances are shown as follows: ↑↑↑/↓↓↓, $p < 0.001$; ↑↑↑↑/↓↓↓↓, $p < 0.0001$

changed significantly when exposed to high pressure and low temperature (Fig. 4B).

The cluster of orthologous groups (COG) annotations of the DEPs were performed using the eggnog website (http://eggnog-mapper.embl.de/), and the results showed that their functions are mainly concentrated in four categories

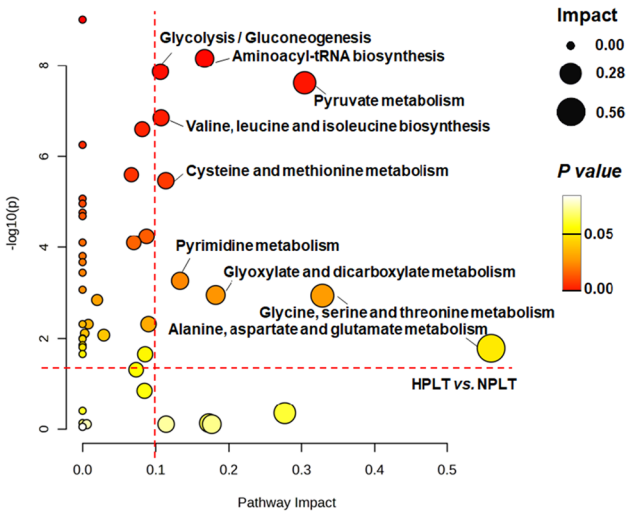

Fig. 3 Metabolic pathway analysis conducted on YLB-01 cells exposed to high-pressure conditions. Significantly altered metabolic pathways were identified with pathway impact value (PIV) > 0.1 and $p < 0.05$, using the pathway analysis module available on the MetaboAnalyst 5.0 webserver

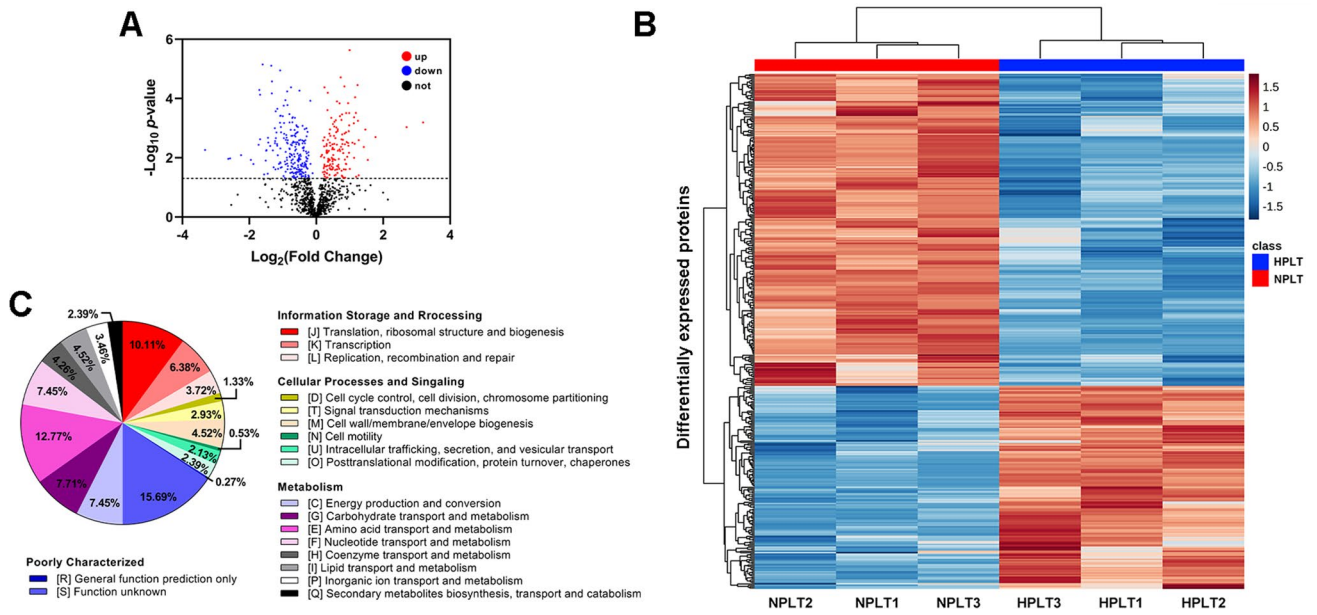

Fig. 4 Identification and functional annotation of differentially expressed proteins. (**A**) Volcano map of DEPs, (**B**) Heatmap of DEPs, (**C**) COG annotation for DEPs. The points above the dashed line correspond to the differentially expressed proteins with $p < 0.05$

(Fig. 4C): information storage and processing (20.21%), cellular processes and signaling (13.83%), metabolism (50.00%), and poorly characterized (15.96%).

To gain further insight into the functional implications of these DEPs, we performed pathway mapping using the KEGG website (https://www.kegg.jp/kegg/mapper/color.html), resulting in the annotation of these DEPs in 95 pathways, as shown in Table S3.

Subcellular localization of differentially expressed proteins

Subcellular localization analysis showed that among the differentially expressed proteins (DEPs), a substantial percentage (62.00%) was predicted to be in the cytoplasm. Additionally, a notable percentage of the proteins were associated with the plasma membrane (25.60%) and cell wall (0.20%), highlighting their roles in cell surface interactions and maintenance of structural integrity. Intriguingly, a small fraction of the proteins (5.40%) was predicted to be secreted extracellularly, suggesting their involvement in intercellular communication and adaptation to the surrounding environment. Moreover, a subset of the proteins (0.80%) was predicted to be expressed in the flagella, indicating their potential contributions to motility and sensing stimuli (Fig. S1). These results revealed the differential expression patterns and subcellular localization of proteins, shedding light on the molecular changes occurring in YLB-01 cells under high-pressure conditions.

Discussion

The deep-sea environment poses many challenges to microorganisms, including low temperature, high pressure, nutrient scarcity, and anaerobic conditions. As water depth increases in the ocean, hydrostatic pressure increases progressively (Saunders and Fofonoff 1976). Previous studies have shown that high-pressure conditions can adversely affect key cellular processes such as DNA stability, ribosome function, and cell membrane fluidity, which are essential for microbial growth in the deep sea (Niven et al. 1999; Wang et al. 2009; Yayanos and Pollard 1969). Elucidating the molecular processes that allow microorganisms to adapt to such extreme conditions is essential to understanding their ability to survive in this inhospitable environment.

It was previously reported that strain YLB-01 could grow in TSB medium at temperatures ranging from 4 °C to 50 °C and pressures from 0.1 MPa to 80 MPa, with the most optimal conditions being 28 °C and 0.1 MPa (Yu et al. 2013). We then conducted further research to examine the growth curves of the YLB-01 strain under different high pressures at both 28 °C and 4 °C. We found that both high pressure and low temperature had a negative effect on the growth of the strain, resulting in a low growth rate and maintaining the initial abundance of the strain for at least one week when exposed to high pressure at low temperature (Fig. S2). To mimic the challenging conditions of the deep-sea high-pressure environment, we designed specific culture conditions, namely HPLT (30 MPa at 4 °C) and NPLT (0.1 MPa at 4 °C). By using an integrative

approach combining NMR-based metabolomics and proteomics analyses, we have elucidated the significantly altered metabolic pathways associated with the adaptation of YLB-01 cells to high-pressure conditions (Fig. 5). Our results revealed substantial modifications in amino acid, carbohydrate, and lipid metabolisms, as well as notable changes in cell wall synthesis and cell membrane fluidity in response to high-pressure conditions. These metabolic adaptations provide the cells with essential mechanisms to thrive in the challenging deep-sea environment.

YLB-01 cells adapt to high pressure by regulating amino acid metabolism

Metabolic pathway analysis of YLB-01 cells revealed a remarkable regulation of amino acid metabolism (e.g., valine, leucine and isoleucine biosynthesis, cysteine and methionine metabolism, glycine, serine and threonine metabolism, and alanine, aspartate and glutamate metabolism), which may be a response to the under high-pressure environment, as indicated by significant changes in amino acid concentrations (Fig. 5). Notably, the high-pressure treatment resulted in increased concentrations of leucine,

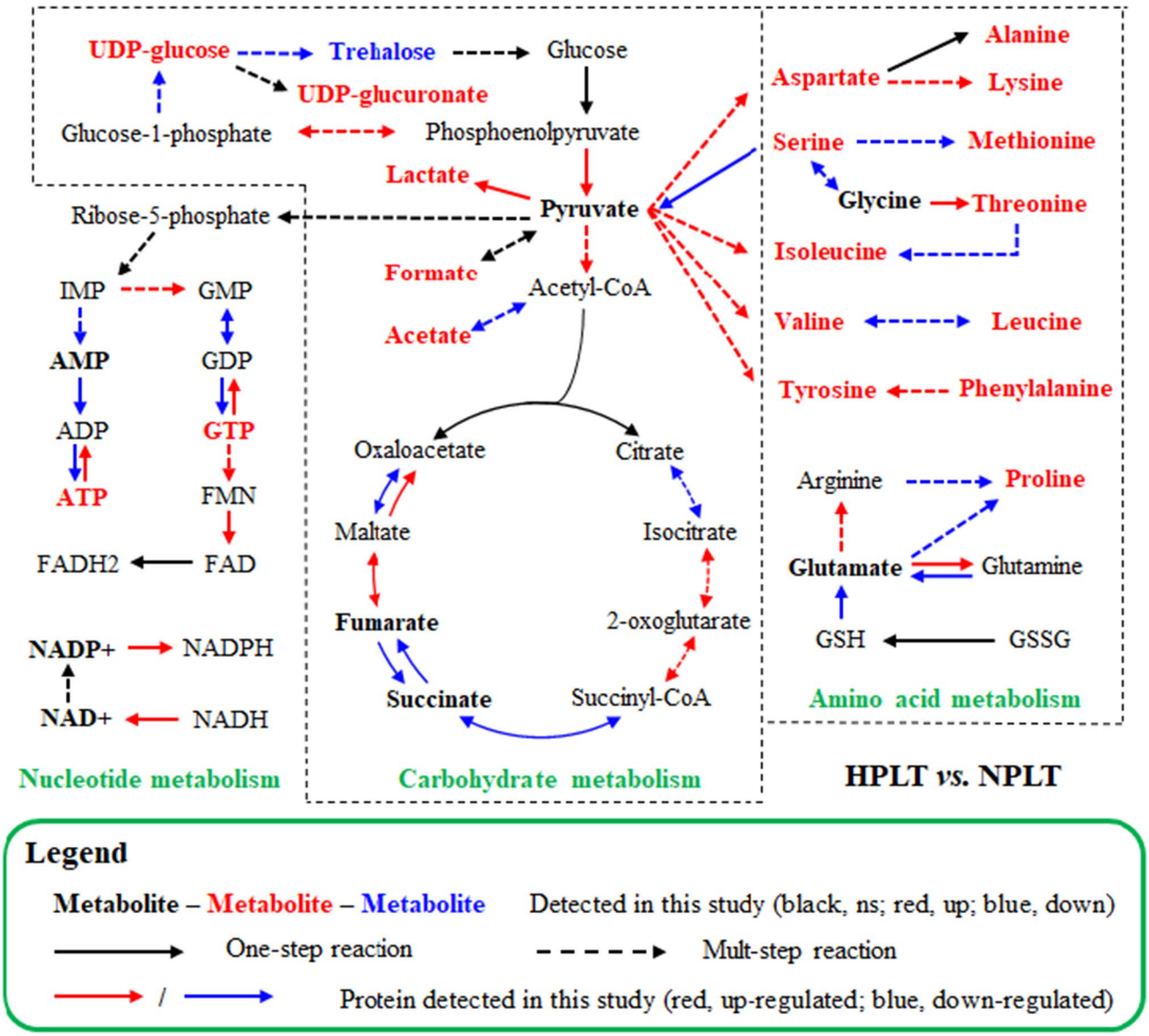

Fig. 5 Significant metabolic pathways identified from the analysis comparing HPLT cells and NPLT cells. The highlighted pathways include the metabolites identified through a comprehensive analysis combining metabolomics and proteomics approaches that were found to be statistically significant ($p < 0.05$). The changing trends in metabolite concentrations and enzyme expressions are indicated for further insights

phenylalanine, tyrosine, and threonine. These results strongly suggest that YLB-01 cells undergo regulatory changes in their amino acid metabolism to adapt to high-pressure conditions.

Previous studies have shown that high pressure-tolerant bacteria, such as strains belonging to *Colwellia*, *Psychromonas*, and *Shewanella*, increase concentrations of basic proteins, that help maintain charge balance within the cytoplasm (Peoples et al. 2020). This phenomenon is likely attributed to the modulation of specific amino acid levels, as the availability of amino acids directly impacts protein composition. Consistent with these findings, our proteomic data showed a significant regulation of amino acid metabolism in YLB-01 cells when exposed to high-pressure conditions (Supplementary Table S2). The observed regulation of amino acid metabolism underlines its crucial role in the adaptive response of YLB-01 cells to the high-pressure environment in the deep sea.

It has also been proposed that stress-tolerant bacteria have higher concentrations of hydrophobic amino acids such as tryptophan, tyrosine, leucine, phenylalanine, histidine, and methionine, whereas pressure-sensitive bacteria have increased levels of glutamate, aspartate, asparagine, and serine (Peoples et al. 2020). Our results are consistent this concept, as YLB-01 cells showed increased levels of hydrophobic amino acids when exposed to high pressure. Furthermore, certain amino acids such as proline and serine are known to act as compatible solutes, allowing YLB-01 cells to survive in extreme environments (Ghobakhlou et al. 2013). These results provide further support for the significant changes in amino acid metabolism observed in YLB-01 cells under high-pressure conditions, highlighting their adaptive capacity and survival mechanisms in the deep sea.

YLB-01 cells adapt to high pressure by promoting carbohydrate metabolism

Our results demonstrate the promotion of carbohydrate metabolism in YLB-01 cells when exposed to high-pressure conditions, similar to the observed effects under low-temperature conditions in the deep sea (Xia et al. 2020). Specifically, we observed significant regulation in key carbohydrate metabolic pathways, such as glycolysis/gluconeogenesis and pyruvate metabolism, in response to high-pressure treatment (Fig. 3). Furthermore, our pathway analysis revealed notable changes in specific metabolites. We observed significantly increased levels of acetate, formate, lactate, UDPG, and UDP-glucuronate, while trehalose levels were significantly decreased. However, the levels of pyruvate and succinate did not show significant changes (Fig. 5). These results highlight the metabolic adaptations of YLB-01 cells to high-pressure conditions, emphasizing the critical role of carbohydrate metabolism in their response to extreme environmental challenges.

In addition, our proteomic analysis revealed the upregulation of the tricarboxylic acid (TCA) cycle and oxidative phosphorylation pathway in YLB-01 cells (Fig. S3), which is consistent with the findings reported by Amrani et al. (Amrani et al. 2014). This finding suggests that microorganisms possess the ability to adapt their energy metabolism by primarily promoting carbohydrate metabolism in response to high-pressure stimulation, thus enabling them to effectively cope with the stress imposed by extreme high-pressure environments. Previous studies have demonstrated that ATP levels in certain pathogenic bacterial cells decrease with increasing environmental pressure or prolonged exposure to pressure (Tholozan et al. 2000; Ukuku et al. 2009). These results provide valuable insights into the molecular mechanisms that enable microorganisms to survive in the deep sea and underscore the crucial metabolic processes that support their thriving in harsh high-pressure conditions.

YLB-01 cells adapt to high pressure by accumulating compatible solutes

Our study showed that strain YLB-01 significantly regulated amino acid and carbohydrate metabolism in response to high pressure, resulting in an increase in several metabolites. Microbes take steps to reduce cell damage when exposed to extreme conditions, which often involves the accumulation of soluble organic compounds (known as compatible solutes) to maintain osmotic balance and protect the cell membrane, proteins, and DNA (Hincha and Hagemann 2004; Lentzen and Schwarz 2006; Muller et al. 2005). Compatible solutes are divided into four categories: carbohydrates, polyols, heterosides, amino acids and derivatives (Vyrides and Stuckey 2017). We hypothesize that the significant upregulation of amino acid and carbohydrate metabolism in strain YLB-01 under high pressure may be related to the formation of compatible solutes.

In response to external stress, many deep-sea microorganisms have been found to produce and secrete compatible solutes, such as proline, alanine, tyrosine, serine and threonine, to maintain osmotic balance and protect their biological macromolecules (Goordial et al. 2016; Mocali et al. 2017; Morawska et al. 2022; van den Berg et al. 2017). Our study showed a significant increase in amino acids after high pressure treatment, with proline being the most significantly increased compatible solute (Table 1). Furthermore, several other amino acids such as alanine, tyrosine, serine, and threonine were significantly enriched. This suggests that strain YLB-01 may adapt to the high-pressure environment by regulating its amino acid metabolism to produce a substantial quantity of compatible solutes.

YLB-01 cells adapt to high pressure by enhancing cell wall synthesis

We observed trehalose was significantly decreased, while UDPG was significantly increased. UDPG serves as a crucial precursor molecule for the synthesis of various cell wall components, particularly polysaccharides. UDPG acts as a substrate for enzymes involved in the biosynthesis of specific cell wall components, such as peptidoglycan, lipopolysaccharides, and glycogen, and therefore plays a critical role in cell wall formation.

To gain further insight into the increased level of UDPG in YLB-01 cells, we analyzed the corresponding proteomic data and found a decrease in the expression of the proteins TPS (Trehalose-6-phosphate synthase) and TPP (Trehalose-6-phosphate), responsible for catalyzing the conversion of UDPG to trehalose, following high-pressure treatment. This decrease in enzyme expression led to the accumulation of UDPG, thereby enhancing cell wall synthesis in YLB-01 cells under high-pressure conditions.

Moreover, the intracellular UDPG level was significantly increased in YLB-01 cells exposed to high-pressure conditions, suggesting that the accumulation of UDPG in response to high-pressure treatment may have a regulatory role in several essential biological processes. Previous studies have demonstrated the involvement of UDPG in the regulation of gene expression of the RNA polymerase S subunit, cell wall synthesis, lipid metabolism, glucose metabolism, amino acid metabolism, and cell respiration (Bohringer et al. 1995; Foulquier and Galinier 2017; Lazarowski et al. 2003; López-Gómez and Lluch 2012). Therefore, our results indicate that the accumulation of UDPG in response to high-pressure treatment plays a critical role in modulating various biological processes in YLB-01 cells.

Although trehalose itself does not directly participate in cell wall formation, its presence and protective functions contribute to the overall health and stability of the cell, indirectly supporting the integrity and functionality of the cell wall. In line with this, we observed a downregulation in the conversion of UDPG to trehalose, as well as a significant decrease in the expression of the protein TreS, responsible for catalyzing the conversion of maltose to trehalose. These results suggest a potential impairment in the protective effect of trehalose on the cell wall of YLB-01 cells exposed to high-pressure conditions.

Our metabolomics analysis revealed a promotion of amino acid metabolism in YLB-01 cells exposed to high-pressure conditions. This metabolic shift could potentially be related to an upregulation of nucleotide metabolism and increased protein synthesis, particularly for cell wall formation. Supporting this, our proteomic data indicated the upregulation of pathways associated with peptidoglycan synthesis in YLB-01 cells under high-pressure conditions. These results suggest that YLB-01 cells adapt to the extreme deep-sea environment by enhancing key processes involved in cell wall synthesis, such as peptidoglycan synthesis, glucose metabolism, and lipid metabolism. This adaptive strategy likely plays a crucial role in the survival of YLB-01 cells in high-pressure environments, highlighting the significance of cell wall synthesis in their adaptation to high-pressure conditions.

YLB-01 cells adapt to high pressure by improving cell membrane fluidity

Hydrostatic pressure exerts a significant influence on the cell membrane of deep-sea bacteria (Michoud and Jebbar 2016). In particular, it leads to a decrease in membrane fluidity, which is crucial for several cellular processes such as nutrient and ion transport, solute uptake, and osmotic pressure regulation (Macdonald et al. 1988). Casadei et al. have shown the close relationship between pressure tolerance and membrane fluidity during the logarithmic growth phase (Casadei et al. 2002). The structural and functional integrity of the cell membrane is highly dependent on its fluidity, which is mainly determined by the fatty acid composition of the membrane (Strahl and Errington 2017). Under high-pressure conditions, the lipid composition of the bacterial cell membrane can be altered, leading to changes in the fatty acid chains within the phospholipid bilayer (Casadei et al. 2002).

Our proteomic analysis revealed interesting changes in YLB-01 cells exposed to high pressure. Specifically, we observed a decrease in the level of long-chain fatty acid CoA and a concomitant increase in the expression of TesB, an enzyme responsible for the conversion of $C_{16:0}$ to palmitic acid. This suggests a shift towards increased fatty acid production and decreased fatty acid consumption, potentially affecting membrane lipid composition. This finding is consistent with previous studies highlighting the importance of ω-3 polyunsaturated fatty acids (PUFAs) in membrane lipids for high-pressure tolerance in pressure-tolerant bacteria (Usui et al. 2012). Notably, Wang et al. showed that cellular concentrations of polyunsaturated fatty acids in the pressure-tolerant bacterium *Sporosarcina* sp. DSK25 increased with elevated hydrostatic pressure (Wang et al. 2014).

Furthermore, our proteomic analysis revealed the upregulation of proteins associated with cell division, indicating active modulation of cell wall components and membrane production by YLB-01 cells in response to high-pressure conditions. This finding aligns with the concept that cells enhance their structural integrity as a protective mechanism in high-pressure environments. Subcellular localization analysis of differentially expressed proteins supports these observations and provides new evidence for the cellular adaptations of YLB-01 cells to thrive in challenging high-pressure

conditions. Our results suggest that YLB-01 cells adapt to high pressure by regulating cell membrane fluidity through alterations in lipid composition and fatty acid metabolism. This adaptive strategy likely plays a pivotal role in enabling YLB-01 cells to withstand the extreme conditions of the deep-sea environment.

YLB-01 cells adapt to high pressure by using mechanisms similar to low temperature

In our previous study of low temperature adaptation for strain YLB-01 (LTHP *vs.* NTHP), we observed distinct metabolic changes in the cells exposed to cold stress at low temperature, particularly in amino acid metabolism and carbohydrate metabolism. Moreover, we observed notable metabolic differences between logarithmic and stationary phase cells cultivated at low temperature compared to those at normal temperature. Specifically, the logarithmic phase cells exhibited suppressed the activity of the TCA cycle, while the stationary phase cells exhibited decreased pyruvate levels and increased lactate production (Xia et al. 2020).

In the present study, we observed a remarkable difference in carbohydrate metabolism between the metabolic adaptation to high pressure and that to low temperature. While low-temperature stress was found to inhibit the TCA cycle in YLB-01 cells, high-pressure stress showed a contrasting effect by significantly promoting the TCA cycle and the oxidative phosphorylation pathway. This upregulation resulted in the accumulation of ATP, suggesting increased energy production and utilization in response to high-pressure conditions.

In our cellular high-pressure stress study, we made a remarkable discovery regarding the levels of UDPG and trehalose in HPLT cells compared to NPLT cells. This is similar to what we observed in our previous cellular low-temperature stress study, where we found that LTHP cells had increased UDPG and decreased trehalose levels compared to NTHP cells (Xia et al. 2020). These consistent results suggest that cell wall formation is an important factor in the metabolic adaptations of YLB-01 cells to both high-pressure and low-temperature conditions in the deep sea.

These contrasting responses to high-pressure stress and low-temperature stress highlight the dynamic and context-dependent nature of metabolic adaptations in YLB-01 cells. The observed differences in the regulatory role of carbohydrate metabolism suggest that YLB-01 cells employ different strategies to cope with the specific challenges imposed by high-pressure stress and low-temperature stress. These results shed light on the complex interplay between cellular metabolism and environmental stress, as well as the mechanisms underlying the survival and adaptation of YLB-01 cells in extreme deep-sea environments.

In summarily, our study has identified several key mechanisms by which YLB-01 cells adapt to high-pressure conditions. These adaptations are crucial for their survival in extreme deep-sea environments. Firstly, YLB-01 cells regulate amino acid metabolism by increasing the levels of hydrophobic amino acids, proline, and serine. This regulation helps maintain osmotic balance and protect cellular structures from the detrimental effects of high pressure. Secondly, YLB-01 cells promote carbohydrate metabolism by enhancing the activity of the tricarboxylic acid (TCA) cycle and the oxidative phosphorylation pathway. This metabolic shift allows for efficient energy production and utilization, supporting cellular functions under high-pressure conditions. Thirdly, YLB-01 cells exhibit enhanced cell wall synthesis by downregulating the conversion of UDPG to trehalose, leading to the accumulation of UDPG. UDPG serves as a precursor molecule for the synthesis of various cell wall components, such as peptidoglycan and lipopolysaccharides. This increased cell wall synthesis strengthens the structural integrity of the cells, enabling them to withstand the challenges of high pressure. Lastly, YLB-01 cells modulate cell membrane fluidity by altering lipid composition and fatty acid metabolism. This adaptive response ensures the optimal functioning of the cell membrane, which is crucial for various cellular processes, including nutrient uptake, ion transport, and osmotic pressure regulation. Overall, these mechanisms collectively contribute to the adaptation of YLB-01 cells to the challenging high-pressure environment in the deep sea. By regulating amino acid metabolism, promoting carbohydrate metabolism, enhancing cell wall synthesis, and modulating cell membrane fluidity, YLB-01 cells can survive in the harsh environment of the deep sea.

It is essential to recognize the restrictions of this study, as it provides valuable guidance for future investigations. Although our results suggest a critical role of UDPG accumulation in the adaptation of YLB-01 cells to high-pressure conditions in the deep sea, further confirmation through knockout assays is warranted to establish a causal relationship. Conducting targeted experiments involving genetic manipulation will provide a more conclusive understanding of the specific contributions of UDPG-mediated adaptation. In addition, to gain a comprehensive understanding of the unique properties and pathways associated with UDPG-mediated adaptation, more extensive investigations are necessary. Exploring the intricate details of UDPG-related processes, such as the enzymatic machinery involved in its biosynthesis and utilization, will offer deeper insights into the molecular mechanisms underlying YLB-01 cells' ability to thrive under high-pressure conditions. Furthermore, although our proteomic analysis revealed the regulatory role of fatty acid metabolism in YLB-01 cells under high pressure, future studies are needed to further investigate lipid metabolism. Investigating the dynamics of lipid composition

and fatty acid profiles in response to high pressure will provide a more comprehensive understanding of the diverse responses of YLB-01 cells to their deep-sea environment. By addressing these aspects, future research can enhance our understanding of the molecular mechanisms underlying the adaptation of YLB-01 cells to high-pressure conditions in deep-sea environments. This knowledge will contribute to a broader comprehension of microbial ecology and the physiological adaptations that enable microorganisms to thrive in extreme environments.

Supplementary Information The online version contains supplementary material available at https://doi.org/10.1007/s00253-023-12906-5.

Author contributions DHL, XXT, and CHH conceived and designed the research. XQ and DHL wrote the manuscript. XQ, XMH and HHJ conducted the experiments and analyzed the data. All the authors have read and approved this manuscript.

Funding This work was financially supported by the National Natural Science Foundation of China (Nos. 31971357, 32271496).

Data availability All data generated or analysed during this study are included in this published article [and its supplementary information files].

Declarations

This article does not contain any studies with human participants or animals performed by any of the authors.

Conflict of interest The authors have declared that no conflict of interest exists.

References

Abe F, Horikoshi K (2001) The biotechnological potential of piezophiles. Trends Biotechnol 19(3):102–108

Amrani A, Bergon A, Holota H, Tamburini C, Garel M, Ollivier B, Imbert J, Dolla A, Pradel N (2014) Transcriptomics reveal several gene expression patterns in the piezophile *Desulfovibrio hydrothermalis* in response to hydrostatic pressure. PLoS One 9(9):e106831. https://doi.org/10.1371/journal.pone.0106831

Bohringer J, Fischer D, Mosler G, Hengge-Aronis R (1995) UDP-glucose is a potential intracellular signal molecule in the control of expression of sigma S and sigma S-dependent genes in *Escherichia coli*. J Bacteriol 177(2):413–422. https://doi.org/10.1128/jb.177.2.413-422.1995

Campanaro S, Vezzi A, Vitulo N, Lauro FM, D'Angelo M, Simonato F, Cestaro A, Malacrida G, Bertoloni G, Valle G, Bartlett DH (2005) Laterally transferred elements and high pressure adaptation in *Photobacterium profundum* strains. BMC Genomics 6:122. https://doi.org/10.1186/1471-2164-6-122

Casadei MA, Manas P, Niven G, Needs E, Mackey BM (2002) Role of membrane fluidity in pressure resistance of *Escherichia coli* NCTC 8164. Appl Environ Microbiol 68(12):5965–5972. https://doi.org/10.1128/aem.68.12.5965-5972.2002

Delong EF, Yayanos AA (1986) Biochemical function and ecological significance of novel bacterial lipids in deep-sea procaryotes. Appl Environ Microbiol 51(4):730–737. https://doi.org/10.1128/AEM.51.4.730-737.1986

Fang J, Zhang L, Bazylinski DA (2010) Deep-sea piezosphere and piezophiles: geomicrobiology and biogeochemistry. Trends Microbiol 18(9):413–422. https://doi.org/10.1016/j.tim.2010.06.006

Foulquier E, Galinier A (2017) YvcK, a protein required for cell wall integrity and optimal carbon source utilization, binds uridine diphosphate-sugars. Sci Rep 7(1):4139. https://doi.org/10.1038/s41598-017-04064-2

Ghobakhlou A, Laberge S, Antoun H, Wishart DS, Xia J, Krishnamurthy R, Mandal R (2013) Metabolomic analysis of cold acclimation of Arctic *Mesorhizobium* sp. strain N33. PLoS One 8(12):e84801. https://doi.org/10.1371/journal.pone.0084801

Goordial J, Raymond-Bouchard I, Zolotarov Y, de Bethencourt L, Ronholm J, Shapiro N, Woyke T, Stromvik M, Greer CW, Bakermans C, Whyte L (2016) Cold adaptive traits revealed by comparative genomic analysis of the eurypsychrophile *Rhodococcus* sp. JG3 isolated from high elevation McMurdo Dry Valley permafrost, Antarctica. FEMS Microbiol Ecol 92(2). https://doi.org/10.1093/femsec/fiv154

Hincha DK, Hagemann M (2004) Stabilization of model membranes during drying by compatible solutes involved in the stress tolerance of plants and microorganisms. Biochem J 383:277–283. https://doi.org/10.1042/Bj20040746

Ishii A, Oshima T, Sato T, Nakasone K, Mori H, Kato C (2005) Analysis of hydrostatic pressure effects on transcription in *Escherichia coli* by DNA microarray procedure. Extremophiles 9(1):65–73. https://doi.org/10.1007/s00792-004-0414-3

Jian H, Xu G, Gai Y, Xu J, Xiao X (2016) The Histone-Like Nucleoid Structuring Protein (H-NS) Is a Negative Regulator of the Lateral Flagellar System in the Deep-Sea Bacterium *Shewanella piezotolerans* WP3. Appl Environ Microbiol 82(8):2388–2398. https://doi.org/10.1128/AEM.00297-16

Lazarowski ER, Shea DA, Boucher RC, Harden TK (2003) Release of cellular UDP-glucose as a potential extracellular signaling molecule. Mol Pharmacol 63(5):1190–1197. https://doi.org/10.1124/mol.63.5.1190

Lentzen G, Schwarz T (2006) Extremolytes: natural compounds from extremophiles for versatile applications. Appl Microbiol Biot 72(4):623–634. https://doi.org/10.1007/s00253-006-0553-9

López-Gómez M, Lluch C (2012) Trehalose and Abiotic Stress Tolerance. In: Ahmad P, Prasad MNV (eds) Abiotic Stress Responses in Plants: Metabolism, Productivity and Sustainability. Springer, New York, New York, NY, pp 253–265

Ma J, Chen T, Wu S, Yang C, Bai M, Shu K, Li K, Zhang G, Jin Z, He F, Hermjakob H, Zhu Y (2019) iProX: an integrated proteome resource. Nucleic Acids Res 47(D1):D1211–D1217. https://doi.org/10.1093/nar/gky869

Macdonald AG, Wahle KWJ, Cossins AR, Behan MK (1988) Temperature, pressure and cholesterol effects on bilayer fluidity; a comparison of pyrene excimer/monomer ratios with the steady-state fluorescence polarization of diphenylhexatriene in liposomes and microsomes. Elsevier 938(2)

Michoud G, Jebbar M (2016) High hydrostatic pressure adaptive strategies in an obligate piezophile *Pyrococcus yayanosii*. Sci Rep 6:27289. https://doi.org/10.1038/srep27289

Mocali S, Chiellini C, Fabiani A, Decuzzi S, de Pascale D, Parrilli E, Tutino ML, Perrin E, Bosi E, Fondi M, Lo Giudice A, Fani R (2017) Ecology of cold environments: new insights of bacterial metabolic adaptation through an integrated genomic-phenomic approach. Sci Rep 7(1):839. https://doi.org/10.1038/s41598-017-00876-4

Morawska LP, Detert Oude Weme RGJ, Frenzel E, Dirkzwager M, Hoffmann T, Bremer E, Kuipers OP (2022) Stress-induced activation of the proline biosynthetic pathway in *Bacillus subtilis*: a population-wide and single-cell study of the osmotically controlled proHJ promoter. Microb Biotechnol 15(9):2411–2425. https://doi.org/10.1111/1751-7915.14073

Muller V, Spanheimer R, Santos H (2005) Stress response by solute accumulation in archaea. Curr Opin Microbiol 8(6):729–736. https://doi.org/10.1016/j.mib.2005.10.011

Niven GW, Miles CA, Mackey BM (1999) The effects of hydrostatic pressure on ribosome conformation in *Escherichia coli*: and in vivo study using differential scanning calorimetry. Microbiology (reading) 145(Pt 2):419–425. https://doi.org/10.1099/13500872-145-2-419

Oger PM, Jebbar M (2010) The many ways of coping with pressure. Res Microbiol 161(10):799–809. https://doi.org/10.1016/j.resmic.2010.09.017

Ohmae E, Gekko K, Kato C (2015) Environmental Adaptation of Dihydrofolate Reductase from Deep-Sea Bacteria. Subcell Biochem 72:423–442. https://doi.org/10.1007/978-94-017-9918-8_21

Parrilli E, Tedesco P, Fondi M, Tutino ML, Lo Giudice A, de Pascale D, Fani R (2021) The art of adapting to extreme environments: The model system *Pseudoalteromonas*. Phys Life Rev 36:137–161. https://doi.org/10.1016/j.plrev.2019.04.003

Peoples LM, Kyaw TS, Ugalde JA, Mullane KK, Chastain RA, Yayanos AA, Kusube M, Methe BA, Bartlett DH (2020) Distinctive gene and protein characteristics of extremely piezophilic *Colwellia*. BMC Genomics 21(1):692. https://doi.org/10.1186/s12864-020-07102-y

Qin Q-L, Wang Z-B, Su H-N, Chen X-L, Miao J, Wang X-J, Li C-Y, Zhang X-Y, Li P-Y, Wang M, Fang J, Lidbury I, Zhang W, Zhang X-H, Yang G-P, Chen Y, Zhang Y-Z (2021) Oxidation of trimethylamine to trimethylamine N-oxide facilitates high hydrostatic pressure tolerance in a generalist bacterial lineage. Science Advances 7(13). https://doi.org/10.1126/sciadv.abf9941

Qiu X, Cao X, Jian H, Wu H, Xu G, Tang X (2022) Transcriptomic Analysis Reveals that Changes in Gene Expression Contribute to *Microbacterium sediminis* YLB-01 Adaptation at Low Temperature Under High Hydrostatic Pressure. Curr Microbiol 79(4):95. https://doi.org/10.1007/s00284-022-02786-9

Saunders PM, Fofonoff NP (1976) Conversion of pressure to depth in the ocean Deep Sea Research and Oceanographic Abstracts 23(1):109-111

Simmons TL, Coates RC, Clark BR, Engene N, Gonzalez D, Esquenazi E, Dorrestein PC, Gerwick WH (2008) Biosynthetic origin of natural products isolated from marine microorganism-invertebrate assemblages. Proc Natl Acad Sci U S A 105(12):4587–4594. https://doi.org/10.1073/pnas.0709851105

Simonato F, Campanaro S, Lauro FM, Vezzi A, D'Angelo M, Vitulo N, Valle G, Bartlett DH (2006) Piezophilic adaptation: a genomic point of view. J Biotechnol 126(1):11–25. https://doi.org/10.1016/j.jbiotec.2006.03.038

Sogin ML, Morrison HG, Huber JA, Mark Welch D, Huse SM, Neal PR, Arrieta JM, Herndl GJ (2006) Microbial diversity in the deep sea and the underexplored "rare biosphere." Proc Natl Acad Sci U S A 103(32):12115–12120. https://doi.org/10.1073/pnas.0605127103

Strahl H, Errington J (2017) Bacterial Membranes: Structure, Domains, and Function. Annu Rev Microbiol 71:519–538. https://doi.org/10.1146/annurev-micro-102215-095630

Tholozan JL, Ritz M, Jugiau F, Federighi M, Tissier JP (2000) Physiological effects of high hydrostatic pressure treatments on *Listeria monocytogenes* and *Salmonella typhimurium*. J Appl Microbiol 88(2):202–212. https://doi.org/10.1046/j.1365-2672.2000.00917.x

Ukuku DO, Zhang H, Bari ML, Yamamoto K, Kawamoto S (2009) Leakage of intracellular UV materials of high hydrostatic pressure-injured *Escherichia coli* O157:H7 strains in tomato juice. J Food Prot 72(11):2407–2412. https://doi.org/10.4315/0362-028x-72.11.2407

Usui K, Hiraki T, Kawamoto J, Kurihara T, Nogi Y, Kato C (1818) Abe F (2012) Eicosapentaenoic acid plays a role in stabilizing dynamic membrane structure in the deep-sea piezophile *Shewanella violacea*: a study employing high-pressure time-resolved fluorescence anisotropy measurement. Biochim Biophys Acta 3:574–583. https://doi.org/10.1016/j.bbamem.2011.10.010

van den Berg J, Boersma AJ, Poolman B (2017) Microorganisms maintain crowding homeostasis. Nat Rev Microbiol 15(5):309–318. https://doi.org/10.1038/nrmicro.2017.17

Vyrides I, Stuckey DC (2017) Compatible solute addition to biological systems treating waste/wastewater to counteract osmotic and other environmental stresses: a review. Crit Rev Biotechnol 37(7):865–879. https://doi.org/10.1080/07388551.2016.1266460

Wang F, Xiao X, Ou HY, Gai Y, Wang F (2009) Role and regulation of fatty acid biosynthesis in the response of *Shewanella piezotolerans* WP3 to different temperatures and pressures. J Bacteriol 191(8):2574–2584. https://doi.org/10.1128/JB.00498-08

Wang J, Li J, Dasgupta S, Zhang L, Golovko MY, Golovko SA, Fang J (2014) Alterations in membrane phospholipid fatty acids of Gram-positive piezotolerant bacterium *Sporosarcina* sp. DSK25 in response to growth pressure. Lipids 49(4):347–356. https://doi.org/10.1007/s11745-014-3878-7

Xia JM, Hu XM, Huang CH, Yu LB, Xu RF, Tang XX, Lin DH (2020) Metabolic profiling of cold adaptation of a deep-sea psychrotolerant *Microbacterium sediminis* to prolonged low temperature under high hydrostatic pressure. Appl Microbiol Biotechnol 104(1):277–289. https://doi.org/10.1007/s00253-019-10134-4

Xiao X, Wang P, Zeng X, Bartlett DH, Wang F (2007) *Shewanella psychrophila* sp. nov. and *Shewanella piezotolerans* sp. nov., isolated from west Pacific deep-sea sediment. Int J Syst Evol Microbiol 57(Pt 1):60–65. https://doi.org/10.1099/ijs.0.64500-0

Xie Z, Jian H, Jin Z, Xiao X (2018) Enhancing the Adaptability of the Deep-Sea Bacterium *Shewanella piezotolerans* WP3 to High Pressure and Low Temperature by Experimental Evolution under H_2O_2 Stress. Appl Environ Microbiol 84(5):1–42. https://doi.org/10.1128/AEM.02342-17

Yayanos AA, Pollard EC (1969) A Study of the Effects of Hydrostatic Pressure on Macromolecular Synthesis in *Escherichia coli*. Cell Press 9(12)

Ye Y, Zhang L, Hao F, Zhang J, Wang Y, Tang H (2012) Global metabolomic responses of *Escherichia coli* to heat stress. J Proteome Res 11(4):2559–2566. https://doi.org/10.1021/pr3000128

Yu L, Lai Q, Yi Z, Zhang L, Huang Y, Gu L, Tang X (2013) *Microbacterium sediminis* sp. nov., a psychrotolerant, thermotolerant, halotolerant and alkalitolerant actinomycete isolated from deep-sea sediment. Int J Syst Evol Microbiol 63(Pt 1):25–30. https://doi.org/10.1099/ijs.0.029652-0

Zhang Y, Li X, Bartlett DH, Xiao X (2015) Current developments in marine microbiology: high-pressure biotechnology and the genetic engineering of piezophiles. Curr Opin Biotechnol 33:157–164. https://doi.org/10.1016/j.copbio.2015.02.013